C.C. Conti, A. Fusetti, A. Spinelli, A. Guardone
Shock Losses and Pitot Tube Measurements in Non-Ideal Supersonic and Subsonic Flows of Organic Vapors
Energy, Vol. 265, 2023, 126087 (10 pages)
doi:10.1016/j.energy.2022.126087

Shock Losses and Pitot Tube Measurements in Non-Ideal Supersonic and Subsonic Flows of Organic Vapors

Camilla C. Conti[a,*], Alberto Fusetti[b], Andrea Spinelli[b], Alberto Guardone[a]

[a] *Politecnico di Milano, Department of Aerospace Science and Technology, via La Masa 34, 20156, Milano, Italy*
[b] *Politecnico di Milano, Energy Department, via Lambruschini 4, 20156, Milano, Italy*

Abstract

The present work documents extensive experimental campaigns involving the first ever L-shaped Pitot tube measurements in non-ideal subsonic and supersonic flows of siloxane MM (hexamethyldisiloxane, $C_6H_{18}OSi_2$), a fluid commonly employed in high-temperature Organic Rankine Cycles (ORCs).
The objective is to establish reliable methodologies for pressure probes usage in flows relevant to ORCs, contributing to power generation efficiency through the improvement of current components design and plant regulation capabilities.
Experimental campaigns were carried out on the Test-Rig for Organic Vapors (TROVA) at Politecnico di Milano, with a total-static Pitot tube designed according to ISO 3966, in non-ideal subsonic flows at Mach numbers $M = 0.2, 0.5$ with total pressure and temperature in the range $P_T = 1 - 7\,\text{bar}$, $T_T = 195 - 205\,^\circ\text{C}$ and a corresponding compressibility factor $Z_T \geq 0.8$. Adequate performance of the complete system was verified and Pitot tube behaviour was found to be unaffected by flow non-ideality, requiring no calibration in the investigated conditions.
A simple Pitot tube was then employed for direct total pressure loss measurements across normal shock waves in non-ideal supersonic flows at $M \simeq 1.5$, with total conditions of $P_T = 1.5 - 12.8\,\text{bar}$, $T_T = 212 - 233\,^\circ\text{C}$ and $Z_T \geq 0.66$. The good agreement between measured losses and theoretical ones calculated from conservation equations attests the validity of the developed methodologies even with supersonic flows.

Keywords: Flow Measurements; Non-Ideal Flows; Pressure Probes; Pitot Tubes; Organic Rankine Cycles.

*Corresponding author
Email address: camillacecilia.conti@polimi.it (Camilla C. Conti)

1. Introduction

Organic Rankine Cycle (ORC) power systems are a variation of the classical steam cycle, in which the working fluid differs from water and can be changed as best suited to the desired application. This additional degree of freedom makes them ideal for power generation from a wide range of heat sources, and more convenient than conventional steam cycles when low to medium source temperature (up to 400 °C) and low to medium power output (up to tens of MW) are considered, thanks to their relatively low cost, plant simplicity and thermodynamic efficiency. ORCs are thus largely employed for power generation from renewable energy sources such as geothermal reservoirs, biomass combustion and waste heat recovery from industrial processes [1, 2, 3]. The latter application is showing the largest growth concerning the number of installed systems, with a $> 200\,\%$ increase between 2016 and 2020 [4], due to rising attention towards energy efficiency for environmental and economic reasons.

ORC applications can be distinguished according to their heat source and temperature ranges into High Temperature (HT-ORCs), with maximum cycle temperature around $300 - 400\,°C$, and Low Temperature (LT-ORCs) cycles, with temperatures below 200 °C. HT-ORCs are normally employed for power generation from solar radiation, biomasses and waste; LT-ORCs are common with geothermal and waste heat from industrial processes or other energy conversion devices (e.g. diesel engines) [5, 6, 7, 8].

The optimal working fluid for thermodynamic efficiency depends on heat source characteristics. For low temperatures, fluids leading to optimal performance are hydrocarbons and halocarbons (e.g., chlorofluorocarbons, hydrochlorofluorocarbons and hydrofluorocarbons) [9, 10, 11, 12, 13, 14]. For high temperatures, optimal fluids are aromatic hydrocarbons, fluorocarbons and siloxanes (i.e. organosilicones constituted by hydrogen/alkyl groups bonded through silicon atoms) [9, 15, 10, 16].

It is thus evident that fluids usually employed in ORCs feature high complexity and molecular weight. Moreover, turbine expansion occurs in the dense gas region near the saturation curve and the critical point, where the well-known ideal gas law is not a suitable description of the involved thermodynamics. As a result of all the above, turbine flows are highly supersonic and show important so-called *non-ideal* flow effects [17], such as the dependance of isentropic expansions on total conditions, analogously to shock waves, whose intensity no longer depends on the pre-shock Mach number only. Accurate design tools accounting for these aspects are necessary in order to achieve high turbine efficiency, which in turn strongly impacts cycle efficiency [1, 2]. Unfortunately, comparison of numerical design and analysis tools, ranging from preliminary loss correlations to full Computational Fluid Dynamics (CFD) simulations, with experiment is relatively rare. This is because detailed experimental data characterizing non-ideal flows for ORC applications is currently not widely available in the open literature due to the intrinsic difficulties in running dedicated experimental facilities. Most high-temperature ORC working fluids are liquids at standard room temperature and pressure, such as siloxanes and some complex hydrocarbons.

Typical inlet turbine flows are instead at saturated, superheated or supercritical conditions, with temperatures and pressures ranging from about 100 to 400 °C and 10 to 50 bar [2]. Thus, to reproduce such conditions in a wind tunnel, a closed gas cycle or a phase transition thermodynamic cycle must be put in place. These are noticeably more complicated and expensive with respect to operation with incondensable gases such as air, where compressed air storage tanks or continuous loops powered by fans or compressors are often sufficient to carry out an experimental campaign. Measurement procedures are also more complex due to high fluid temperature and possible condensation issues in pneumatic lines. Moreover, the non-ideal flow field dependance on stagnation conditions significantly increases the number of flows to be experimentally reproduced for a complete characterization of the fluid behavior.

Despite these difficulties, several active plants are starting to provide valuable experimental data on relatively simple yet extremely useful geometries such as converging-diverging nozzles. These allow to reproduce elementary flows important for fundamental fluid dynamics studies and are also the simplest geometry representative of blade passages in ORC turbines. Amongst these so-called nozzle-fitted facilities is the Test Rig for Organic VApors (TROVA) [18] at the Laboratory of Compressible Fluid-dynamics for Renewable Energy Applications (CREA Lab) of Politecnico di Milano, where all the experimental campaigns concerning the present work were carried out. Other plants of this kind are the ORCHID at TU Delft [19], the CLOWT at Muenster University of Applied Sciences [20] and the dense-gas blowdown facility at Imperial College London [21]. Several turbine-fitted facilities mainly devoted to performance measurement of the different components and of the overall thermodynamic cycle also exist, such as the LUT micro-ORC test rig at Lappeenranta – Lahti University of Technology [22]. The ORCHID at TU Delft is designed to also operate with a turbine instead of a nozzle.

Due to the peculiarities of non-ideal vapor flows in ORCs, measurements such as velocity magnitude and direction, mass flow rate or turbine performance, which are routinely carried out in more standard cycles and turbomachinery (e.g., gas turbines operating with air and combustion gases), are not often performed yet. For example, a relevant issue in real operating plants is indeed the closure of mass and energy balances due to the lack of reliable mass flow rate measurements [23], hindering the fine regulation of single components and of the overall cycle, and thus impacting on power generation efficiency. All of this is mainly because specific measurement methods have not been experimentally verified and validated, also considering that no appropriately calibrated instrumentation for non-ideal conditions is currently available. Indeed, none of the previously mentioned wind tunnels for non-ideal flows is routinely employed as a dedicated calibration facility for pressure probes.

Research efforts are now starting to move towards this direction. Results on the performance of a rotable cylinder Pitot probe in high subsonic flows with fluid Novec^{TM} 649 at the CLOWT plant were published [24] as part of a preliminary study to establish measurement techniques for determination of Mach numbers in high-subsonic and transonic organic vapor flow fields.

Considering all the above, even blade cascade testing, quite common in the design process of gas and steam turbines, is instead significantly more complex in the case of non-ideal flows due to the mentioned difficulties in running dedicated wind tunnels and the lack of established probe measurement methodologies. To the Authors' knowledge, the first experimental campaign of this kind was carried out at Whittle Laboratories of Cambridge University in a newly modified transient wind tunnel of Ludwieg tube-type, where annular turbine cascade flows of R134a were characterized with pressure measurements [25]. Wake measurements of R134a flows in the same cascade were performed with a wedge total pressure probe with substantial complementary use of CFD calculation. The latter was necessary to overcome the unavailability of a Mach number measurement upstream of the probe allowing to calculate shock losses at the probe tip in order to retrieve the pre-shock total pressure and evaluate cascade losses [26]. Linear blade cascade testing was recently carried out in the CLOWT facility at Muenster University in order to verify theoretical predictions of critical and choking Mach numbers of organic vapor flows [27].
With the objective of measuring cascade losses to validate low and high-fidelity turbine design tools, a linear cascade experiment representative of the stator operation of axial/radial turboexpanders for ORC systems will be concluded in the very near future at the *TROVA* wind tunnel at CREA Lab of Politecnico di Milano with fluid siloxane MM [28].

The research effort documented in this paper represents a contribution to the development of measurement systems and practices for a reliable use of pressure probes operating with non-ideal flows of interest in the ORC field. As a starting point, L-shaped Pitot-type probes were chosen because they are the simplest instrument giving a fairly straighforward determination of flow velocity and flow rate, allowing immediate transposition in industrial applications. If designed according to geometrical proportions recommended in the reference standard ISO 3966 [29] and employed in subsonic incompressible conditions (Mach number $M \leq 0.25$), calculation of flow velocity follows directly from the probe total and static pressure measurements without the use of calibration coefficients. In case of subsonic compressible flow with $0.25 \leq M \leq 0.80$, calibration in the desired operating conditions is recommended and expressions based on ideal gas isentropic flow are provided in the norm for the compressibility correction factor. The latter accounts for flow Mach number and fluid type through the ideal gas specific heats ratio γ, meaning that non-ideality is overall not considered in this standardized methodology. A first contribution of the present work is to indeed evaluate the performance of a standard-design Pitot tube in non-ideal compressible subsonic flows of fluids that are significantly different than common air or water, and investigate the possible need for calibration coefficients. To the Authors' opinion, this is a necessary learning step towards the calibration in non-ideal flows of the more complex directional pressure probes usually involved in research-oriented studies, further justifying the choice of Pitot-type probes as the basis for future developments in the field of experimental non-ideal fluid dynamics.
The experimental campaigns here reported were carried out on the TROVA

using siloxane MM (hexamethyldisiloxane, $C_6H_{18}OSi_2$) as working fluid. Siloxanes are commonly employed in high temperature ORC plants and also present some favorable properties that make them particularly suitable for research activities. They are characterized by reasonable critical temperatures ($240\,°C < T_c < 420\,°C$) with relatively low critical pressure ($7\,bar < P_c < 20\,bar$), allowing the study of the region near the critical point where non-ideality effects become more significant with the use of a relatively simple experimental setup with manageable technical challenges. Moreover, siloxanes show good thermal stability [30, 31], are non-toxic and only weakly flammable, in addition to being easily available at a fairly low cost due to their widespread usage in plastics and cosmetics industries.

Subsonic testing was carried out in conditions representative of measurement sections in real ORC plants where Pitot tubes can be employed for mass flow rate and overall performance measurement.

Supersonic testing was also performed to measure directly, for the first time ever, total pressure losses across shocks of non-ideal flows of MM vapor. Investigated conditions of temperature, pressure and Mach number were representative of the flow downstream of ORC turbines stator cascades where Pitot tubes can be used for measurement of interstage losses, thus setting the foundations for future testing of blade cascades operating with such flows.

Overall, the current lack of consolidated measurement practices in non-ideal flows is an obstacle for further improvements in components design and plant regulation capabilities, compounding to a limitation in power generation efficiency in organic Rankine cycles. The present research is thus motivated by the mission of improving renewable power generation performance, with the goal of providing tools and methodologies for reliable flow measurements with pressure probes in non-ideal flows. This will enable better machinery and plant design, regulation and management in the field of power generation from ORCs, and even in other key technologies for decarbonization involving unconventional fluids in non-ideal conditions, like heat pumps, CO_2 capture & storage and the hydrogen value chain.

The paper is structured as follows. Section 2 describes the working principles of the TROVA experimental facility, its components and instrumentation. Section 3 details the pneumatic system implemented for pressure probe measurements in the TROVA. Section 4 reports experimental results of subsonic Pitot tube measurements and Section 5 documents direct total pressure loss measurements across shocks in non-ideal flows of siloxane MM. Section 6 draws the conclusions of this work and suggests future outlooks.

2. Experimental Setup

2.1. Test Rig for Organic VApors - TROVA

The *Test Rig for Organic VApors* (TROVA) is a blowdown wind tunnel built with the aim of characterizing non-ideal flows of organic vapors representative of turbine expansions in ORCs.

The working fluid is isochorically heated in a High-Pressure Vessel (HPV) until desired temperature and pressure are reached. It is then discharged to a Low-Pressure Vessel (LPV) by passing through a settling chamber (plenum) and expanding in the test section through a purposely designed planar nozzle.
TROVA operation is intrinsically transient due to its batch nature. Before the beginning of a test, the test section and LPV are vacuumized to working fluid saturation pressure at room temperature ($P \sim 50\,\text{mbar}$ for siloxane MM). After test start, a peak is reached and then pressure decreases in time with a low frequency content ($\sim 1\,\text{Hz}$) related to the emptying of the HPV [32]. Due to the decreasing pressure linked to the plant batch nature, the most non-ideal flow conditions are achieved at the beginning of each test.
More detail on TROVA design and operation can be found in [18].

2.2. Nozzle Expansion Characterization and Instrumentation

Flow expansions are characterized by total conditions measurements in the plenum upstream of the test section, where velocity is low enough (about 1 m/s) for kinetic energy to be negligible. Thus, total pressure P_T is measured at a wall tap with an absolute pressure transducer and total temperature T_T with thermocouples. Total temperature and pressure can vary in the range $200 - 260\,^{\circ}\text{C}$ and $0.5 - 24\,\text{bar}$ respectively for fluid MM.
Nozzle flow is characterized by static pressure measurements at wall taps of 0.3 mm in diameter machined on the rear plate of the test section along the nozzle axis. Absolute piezoresistive transducers are flush-mounted and are directly exposed to high temperature organic vapor flows. Due to their intrinsic temperature sensitivity, transducers must be calibrated both in pressure and temperature from vacuum to full scale ($3.5\,\text{bar} \leq FS \leq 40\,\text{bar}$) and in the range $25 - 300\,^{\circ}\text{C}$. Thermocouples are calibrated in the same temperature range. The expanded uncertainty is 0.07 % of the full scale for pressure sensors and about $1\,^{\circ}\text{C}$ for thermocouples. Discrete pressure measurements in supersonic conditions are supported by schlieren visualizations. Details on the optical apparatus and further information on *TROVA* instrumentation can be found in [32].
The total-static Pitot tube shown in Figure 1, with a head length of 25 mm, outer diameter of 1.6 mm, total pressure tap diameter of 0.6 mm and six taps on the static ring, was employed in subsonic testing. Geometrical proportions are compliant to guidelines indicated in ISO 3966 [29].
The simple Pitot tube (a total pressure probe) in Figure 2, with a head length of 35 mm, total pressure tap diameter of 0.6 mm and outer diameter of 1.6 mm was instead used for shock loss measurements in supersonic flow.

2.3. Nozzles

Planar choked converging nozzles are used in the present work as a subsonic wind tunnel for Pitot tubes in non-ideal flows. They are characterized by a portion with constant cross-sectional area yielding design Mach numbers of 0.2 and 0.5, and are named accordingly as *cMM02* and *cMM05* as illustrated in Figure 3. The first convergent section is determined by a 5th order polynomial, yielding a double concavity that provides gentle flow acceleration up to the defined

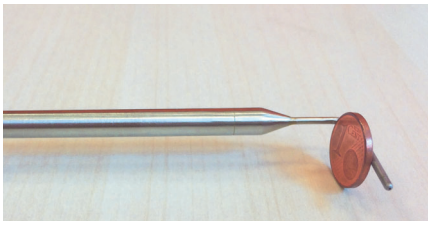

Figure 1: Total-static Pitot tube employed in subsonic testing.

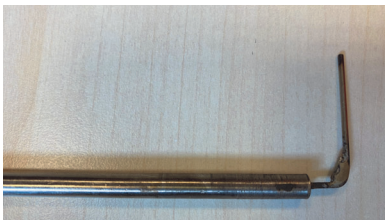

Figure 2: Simple Pitot tube (total pressure probe) employed in supersonic testing.

Mach number and reduces flow non-uniformity. This portion and the constant cross-section one (semi-height $h = 19\,\text{mm}$) are the same for both nozzles. The profile of the second convergent is a straight line that ends at the throat, which is always choked due to the very low pressure in the LPV. The slope of this straight line is the same for both *cMM02* and *cMM05*, but the length is such that the area ratio between throat and constant cross-section corresponds to the desired Mach number at design total conditions $P_T = 5\,\text{bar}$ and $T_T = 210\,^\circ\text{C}$. Therefore, nozzle *cMM05*, shown in red in Figure 3, is shorter and features a larger throat area compared to nozzle *cMM02*, in blue.

The Pitot tube insertion point was determined so that the probe tip is in the middle of the constant cross-section region. Pressure tap 1 is located at the end of the first converging section, while taps 2, 3 and 4 are all positioned in the constant cross-section portion and are basically equally spaced upstream of the probe stem. Tap 3 is in correspondence of the Pitot tube tip and tap 4 is aligned with the static pressure ring.

This nozzle design allows the evaluation of Pitot tube static pressure measurements by direct comparison of pressure measured by the probe static ring with pressures measured at adjacent pressure taps 2, 3 and 4. Indeed, compared measurement points are all located in the constant cross-section portion of the nozzle, so the same pressure should be found.

A front view of the test section with nozzle *cMM02* and inserted total-static Pitot tube is reported in Figure 5.

Planar converging-diverging nozzle *nW-M15* in Figure 4 was instead employed for supersonic Pitot tubes testing at Mach number $M \sim 1.5$. The convergent part was designed according to the same procedure used for subsonic nozzles. The diverging portion shape was determined through the method of characteristics, implemented according to Zucrow and Hoffman [33], coupled with a suitable thermodynamic model for non-ideal gases [34] to deliver a uniform Mach number and a velocity parallel to the nozzle axis at the exit section. Further design details can be found in [35]. In this case, the static pressure measured at the last tap fs in Figure 4, located only a few millimeters ($3 - 4\,\text{mm}$) upstream of the probe tip, is representative of the free-stream one impinging on the Pitot tube.

A front view of the test section with nozzle *nW-M15* and inserted total pressure

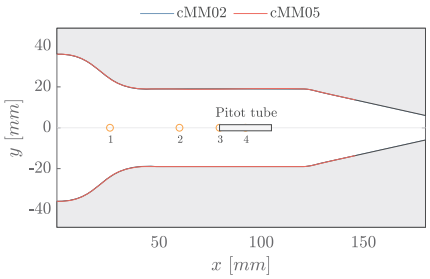

Figure 3: Subsonic choked nozzles with pressure taps (1,2,3 and 4).

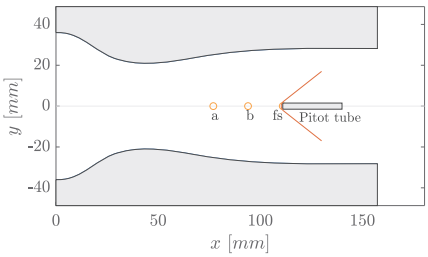

Figure 4: Nozzle with pressure taps (a,b and free-stream fs) and Pitot tube with a bow shock sketch.

Figure 5: Front view of the test section with planar choked nozzle *cMM02* and inserted total-static Pitot tube.

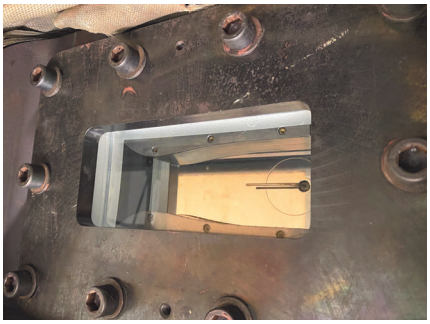

Figure 6: Front view of the test section with planar converging-diverging nozzle *nW-M15* and inserted total pressure probe.

probe can be found in Figure 6.

For all nozzles, depth is imposed by the test section to 18.7 mm.

3. Pneumatic Lines

When probes are employed, differential pressure measurements are carried out between the various probe taps or between a probe tap and the respective plant reference quantity in order to minimize the final measurement uncertainty. This requires the use of pneumatic lines.

Since siloxane MM is liquid at room temperature and considered operating pressures during tests, unheated pneumatic lines are subject to condensation. This can lead to poor measurements quality related to presence of vapor-liquid menisci, hydrostatic head, and time delay due to mass-sink effects.

A pneumatic lines scheme involving nitrogen flushing was purposely developed and implemented to allow probes insertion in the plant test section whilst avoiding the above issues (more detail can be found in [36]). As illustrated in Figure 7, the system is directly connected to nitrogen storage tanks and pressure is

regulated through a pressure reducer to just above the maximum expected one during the test. Electro valves are actuated by a *Labview*® program to open as the test is triggered and close right after the pressure peak is reached in the test section. This ensures that each line only contains nitrogen at all times during a test and no MM vapor enters it, so as to avoid condensation. As the test proceeds, nitrogen exits the line through the static tap into the test section as line pressure is in equilibrium with the decreasing test section one.
Particular care was taken during system design and components positioning to minimize lines length and fittings volume, so as to decrease the overall response time as much as possible. The complete pneumatic lines configuration for subsonic probes testing here presented is specifically devised so that each quantity measured by the probe can be compared against plant references, allowing to evaluate the system behavior. The quantities of interest to be measured during TROVA testing of Pitot tubes in subsonic flows of Siloxane MM are:

- $P_{t,ref}$: reference total pressure in the TROVA plenum, measured with a flush mounted absolute transducer;
- $P_{s,ref}$: reference static pressure in the constant cross section part of the subsonic choked nozzle, measured with a flush mounted absolute transducer at tap number 2 in Figure 3;
- $P_{t,line}$: total pressure measured in the line exiting a pressure tap in the plenum;
- $P_{s,line}$: static pressure measured in the line exiting wall tap number 4 in the constant cross-section region of the nozzle in Figure 3, in correspondance of the Pitot tube static ring;
- $P_{t,pitot}$: total pressure measured in the line connected to the total pressure port of the Pitot tube;
- $P_{s,pitot}$: static pressure measured in the line connected to the static ring of the Pitot tube;
- $\Delta P_{ts,line}$: reference kinetic head directly measured with a differential transducer between a total pressure tap in the plenum and static wall tap number 4 in Figure 3.
- ΔP_t: total pressure difference directly measured with a differential transducer between the pressure tap in the plenum and the Pitot tube one;
- ΔP_s: static pressure difference directly measured with a differential transducer between static wall tap number 4 and the Pitot tube one;
- $\Delta P_{ts,pitot}$: kinetic head directly measured with a differential transducer by the Pitot tube.

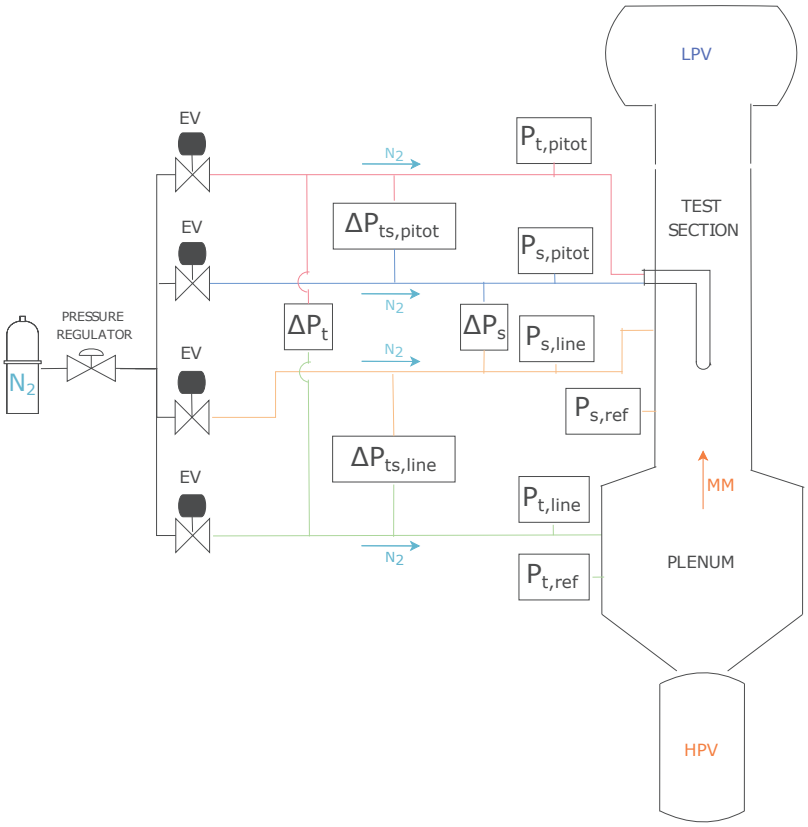

Figure 7: Flushed pneumatic lines scheme for Pitot tube testing in subsonic flows of Siloxane MM. Rectangular boxes represent pressure transducers.

The last four quantities are acquired in differential mode to minimize measurement uncertainty, as previously mentioned. Absolute transducers on each line are used as support to pinpoint any possible measurement issues.

The pneumatic system for measurements in supersonic conditions is simpler. Compared to the complete subsonic configuration, only the difference ΔP_t between the plenum total pressure (upstream of the shock) and the probe total pressure (downstream of the shock) is of interest here. Quantity ΔP_t is now a direct measure of the total pressure loss across the shock. Absolute transducers are still present on each line to help with possible issues identification.

For both subsonic and supersonic testing, employed differential transducers are from *Schaevitz P2100* and *Kulite XTL-3-375(M)* series, with full scale chosen in the range $0.7-5.9$ bar (uncertainty range $1.7-3.3$ ‰ of the full scale) according to the expected measured pressure difference.

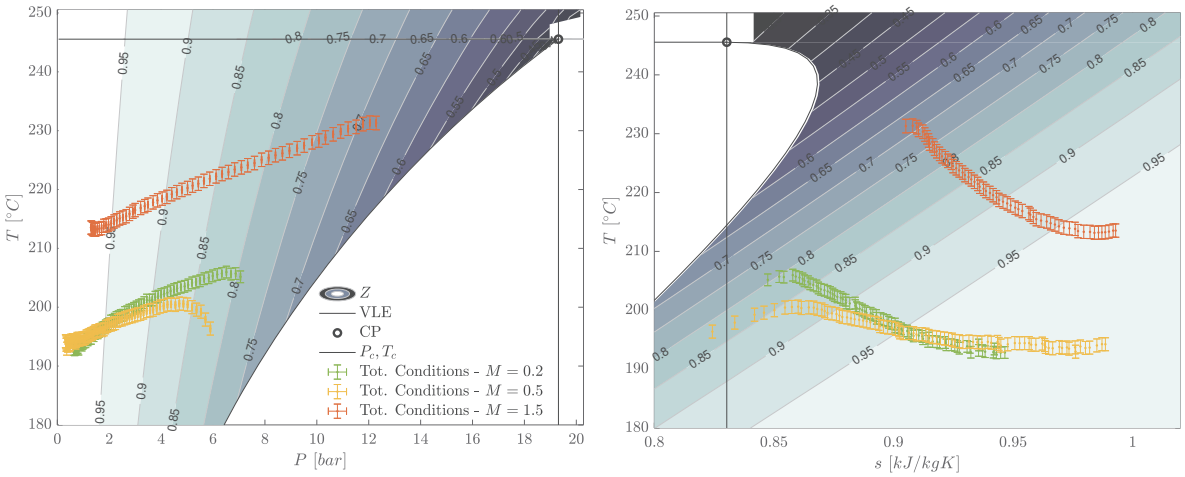

(a) Total conditions reported on the temperature-pressure thermodynamic diagram for siloxane MM.

(b) Total conditions reported on the temperature-specific entropy thermodynamic diagram for siloxane MM.

Figure 8: Evolution of total conditions during exemplary tests at each considered Mach number. In both plots, Z is the contour of compressibilty factor, *VLE* is the Vapor-Liquid Equilibrium curve, *CP* is the Critical Point and P_c, T_c are critical pressure and temperature, respectively.

4. Pitot Tube Measurements in Non-Ideal Subsonic Flows

Pitot tubes testing in non-ideal subsonic MM flows involved about 30 runs with *cMM02* and *cMM05* at total conditions at the beginning of the test of $P_T = 6 - 7\,\text{bar}$, $T_T = 195 - 205\,^\circ\text{C}$, evolving towards dilute conditions of $P_T \simeq 1\,\text{bar}$ and $T_T \simeq 195\,^\circ\text{C}$ at the end.

Repeated testing showed good consistency and reliability of results.

Figure 8 reports the evolution of total conditions during exemplary tests at each considered Mach number, plotted in temperature-pressure (Figure 8a) and temperature-specific entropy (Figure 8b) thermodynamic diagrams for siloxane MM, with compressibility factor Z contours. The two plots illustrate the investigated total conditions which, for subsonic testing, range from mildly non-ideal, with compressibility factor at total conditions $Z_T \simeq 0.8$ closer to the saturation curve, to ideal gas-like at $Z_T \simeq 0.98$.

To analyze subsonic test results, data from only one exemplary run at nominal Mach number $M = 0.5$ is reported in Figure 9a to Figure 9d, for brevity.

All acquired absolute pressures are plotted as a function of time in Figure 9a. The reference total pressure $P_{t,ref}$ measured with a flush-mounted transducer is superposed to $P_{t,line}$ and $P_{t,pitot}$. The total pressure difference ΔP_t, directly measured with a differential transducer, is never larger than 7 mbar. This is evident in Figure 9c, where ΔP_t is reported together with pressure computed from absolute transducers. All three quantities agree, although the calculated pressure differences have a very large errorbar due to the large uncertainty prop-

agated from absolute measurements. This highlights the importance of using differential transducers instead of absolute ones in the present case.

Quite analogously, the three measured static pressures $P_{s,ref}$, $P_{s,line}$ and $P_{s,pitot}$ in Figure 9a are also superposed. Consistently, the static pressure difference ΔP_s in Figure 9d is always well below 3 mbar and its trend agrees very well with the difference between absolute transducers. Given the good measurement performance in both total and static quantities, the kinetic head reported in Figure 9b shows a perfect overlap between readings from all differential and absolute transducers.

In percentage terms with respect to the kinetic head, differences between Pitot tube and TROVA reference quantities are always below 3% for total pressure and 1.5% for static pressure for all Mach numbers. These values are fairly constant during all tests and in line with findings from a preliminary characterization in air (not reported here for brevity), indicating an adequate performance of the complete pneumatic system in non-ideal subsonic flows of siloxane MM for total, static and kinetic head measurements. From these findings, it can be concluded that fluid type and level of flow non-ideality do not significantly affect probe behavior in the investigated range of operating conditions. No particular calibration is thus required for the considered Pitot tube, designed according to ISO 3966 [29]: the instrument total, static pressure and/or kinetic head readings can be simply coupled with a total temperature measurement and a suitable thermodynamic model to calculate isentropic expansions in order to determine flow quantities, including local velocity, density and Mach number. This provides extremely useful information for direct Pitot tubes employment in engineering processes involving non-ideal flows.

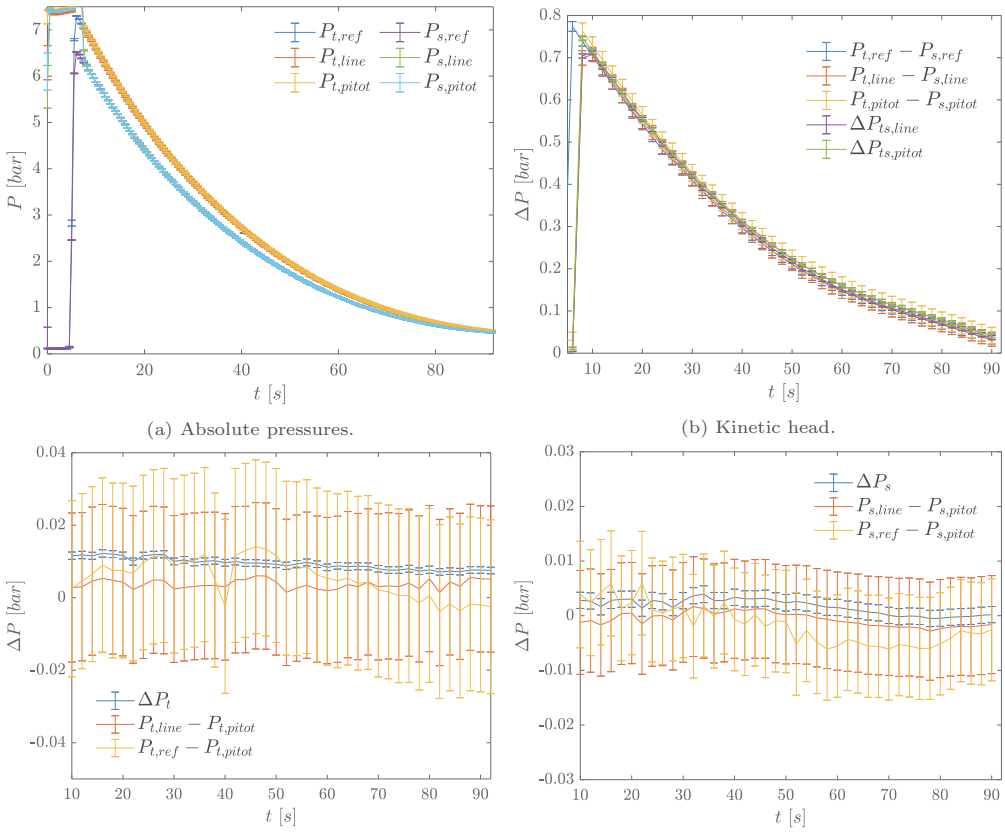

(a) Absolute pressures.

(b) Kinetic head.

(c) Total pressure difference.

(d) Static pressure difference.

Figure 9: Measured pressures during Pitot tube subsonic testing with nozzle *cMM05* at Mach number $M = 0.5$.

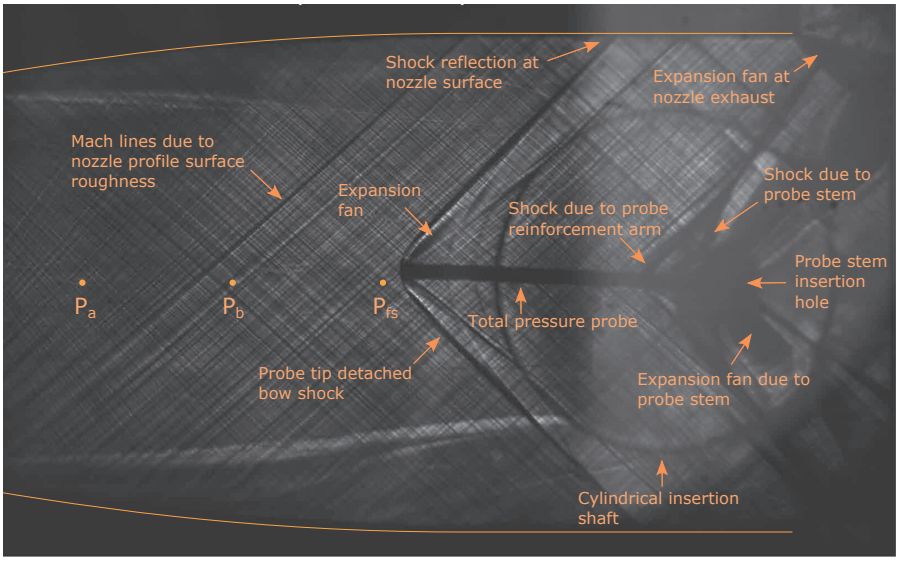

Figure 10: Schlieren image from an exemplary TROVA test for direct total pressure loss measurements across normal shocks in non-ideal flows of siloxane MM vapor at Mach number $M \simeq 1.5$. Nozzle contour, pressure taps and main flow features are highlighted.

5. Shock Loss Measurements In Non-Ideal Supersonic Flows

The first ever direct total pressure loss measurements across normal shocks in non-ideal flows of siloxane MM vapor are here reported. As reported in Figure 8, signficantly non-ideal initial total conditions of $P_T = 12.8\,\text{bar}$ and $T_T = 233\,^\circ\text{C}$ ($Z_T \simeq 0.66$) were considered for the present experimental campaign with a pre-shock Mach number $M \simeq 1.5$, reaching dilute conditions of $P_T = 1.5\,\text{bar}$ and $T_T = 212\,^\circ\text{C}$ ($Z_T \simeq 0.98$) at the end of the test.
Data consistency was verified by test repetition, and results from one exemplary run are reported here only.
The schlieren image of the nozzle divergent in Figure 10 shows that the wind tunnel operating regime is the expected one, with supersonic flow impinging on the probe tip resulting in a bow shock that is locally normal to it. Figure 11 reports all measured pressures during the test, labelled according to pressure taps in Figure 4 and to the pneumatic system scheme in Figure 7. Pressure $P_{t,line}$ is in perfect agreement with the reference total pressure in the plenum $P_{t,ref}$ after line flushing has ended, indicating no issues on the upstream total pressure line to the differential transducer. The two pressures are within error bars of one another from test time $t = 7\,\text{s}$, so less than $0.4\,\text{s}$ after peak pressure was reached. The absolute total pressure measured by the Pitot tube $P_{t_2,pitot}$ is compared to the theoretical post-shock total pressure $P_{t_2} - nIG\,P_{fs,exp}$ calculated from experimental total conditions and free-stream pressure P_{fs} measured at the last tap just before the probe, assuming a normal shock at the probe tip

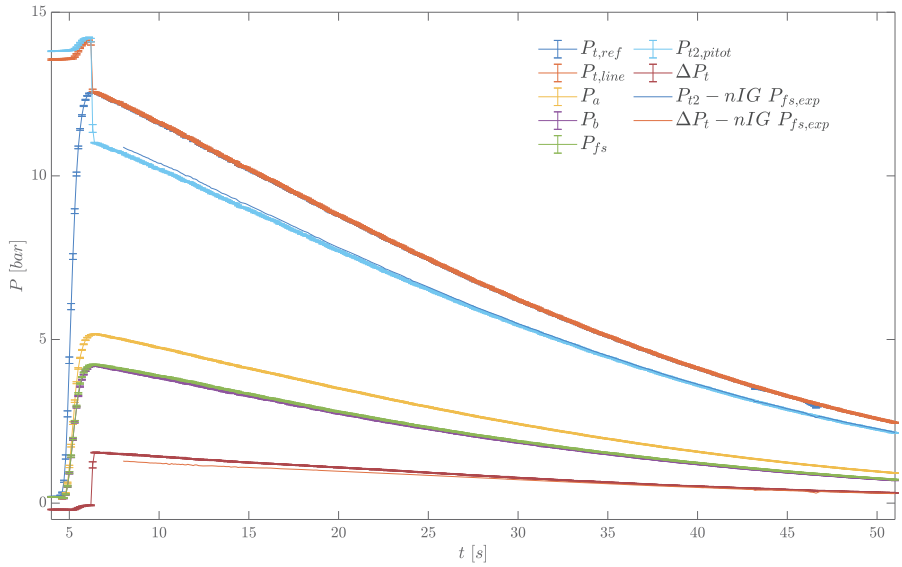

Figure 11: Pressures during an exemplary TROVA test for direct total pressure loss measurements across normal shocks in non-ideal flows of siloxane MM vapor at Mach number $M \simeq 1.5$.

and by numerically solving mass, momentum and energy conservation equations across the shock coupled with the Span-Wagner thermodynamic model [37] embedded in the FluidProp library [38]. The latter is a state-of-the-art multiparameter model able to provide accurate thermodynamic properties even close to the critical point. A functional form for the fundamental relation, linking all thermodynamic properties of a simple system in a stable equilibrium state, is provided in terms of the reduced Helmoltz free energy as a function of the inverse reduced temperature and reduced density [37]. For siloxane MM, implemented model parameters were first presented in [39, 40] and were more recently improved by [41, 42].

The set of equations to be solved are thus the three conservation equations coupled with the enthalpy equation given by the thermodynamic model:

$$\rho_1 u_1 = \rho_2 u_2 \quad (1)$$

$$\rho_1 u_1^2 + P_1 = \rho_2 u_2^2 + P_2 \quad (2)$$

$$h_1 + u_1^2/2 = h_2 + u_2^2/2 \quad (3)$$

$$h_2 = h(P_2, \rho_2) \quad (4)$$

where ρ is density, u velocity, P pressure, h enthalpy and subscript 1 indicates static pre-shock quantities while subscript 2 static post-shock ones. Pre-shock values of velocity, density and enthalpy are calculated from total pressure, total temperature and free-stream pressure P_{fs} by assuming an isentropic expansion in the nozzle and using the thermodynamic model.

Shock loss calculation is initialized imposing the polytropic ideal gas solution and a numerical result for post-shock values is achieved by iterating on variable ρ_2. Once post-shock static quantities are determined, post-shock total enthalpy is calculated as $h_{t_2} = h_2 + u_2^2/2$ and total pressure follows from the thermodynamic model as $P_{t_2} = P(h_{t_2}, s_2)$, where $s_2 = s(P_2, \rho_2)$ is post-shock entropy. The agreement between experimental and calculated post-shock total pressure is satisfactory considering that discrepancies are always below 2% with respect to the measured $P_{t_2,pitot}$.

Figure 11 also reports total pressure loss across the shock ΔP_t directly measured with the differential transducer, together with the total pressure difference $\Delta P_t - nIG\, P_{fs,exp}$ calculated consistently with $P_{t_2} - nIG\, P_{fs,exp}$ above. The calculated pressure drop is always lower than the experimental value. At $t = 10s$ the difference between the two is 200 mbar, decreasing to 75 mbar at $t = 25$ s and to 20 mbar at $t = 50$ s. Whilst these are not negligible discrepancies in absolute terms, they are a satisfactory result in percentage terms, with differences that are only 3% of the pre-shock kinetic head at test start, down to 1% at the end of the test.

6. Conclusions and Outlook

The present work reports results from extensive experimental campaigns involving the first ever L-shaped Pitot tube measurements in non-ideal subsonic and supersonic flows of siloxane MM vapor, with the objective of establishing reliable methodologies for pressure probe measurements in flows of interest for organic Rankine cycles. This will contribute to the improvement in current components design and plant regulation capabilities, helping increase renewable power generation efficiency.

A pneumatic lines scheme involving nitrogen flushing was purposely designed and implemented to allow probes insertion in the test section of the Test Rig for Organic VApors (TROVA) blow-down wind tunnel at Politecnico di Milano whilst avoiding issues linked to possible condensation. Pitot tube testing in subsonic flows at Mach numbers 0.2 and 0.5 allowed to verify the adequate performance of the complete pneumatic system and procedures in non-ideal subsonic flows of siloxane MM for total, static and kinetic head measurements. Moreover, Pitot tube behaviour was found not to be affected by the level of flow non-ideality, indicating that no calibration is required for this type of instrument (designed according to ISO 3966 [29]) in the investigated subsonic conditions, common in ORC plants measurement sections where Pitot tubes can be directly exploited for velocity and mass flow rate measures, allowing an immediate transposition of the results of this research in the industrial field. In this respect, for the general power generation and management field, it would be of interest to experimentally verify the performance of other differential pressure devices usually employed in steam, gas and oil & gas plants for flow rate measurements (e.g., orifice plates and Venturi tubes), with fluids different than

air, steam and natural gas. Indeed, common practice as suggested in the reference standard ISO 5167 [43], is to implement a formulation for the expansibility factor of the instrument (accounting for compressiblity effects) based on experimental test results with these three fluids, and employ it for use with any other gas/vapor by considering the value of the isentropic exponent. The latter depends on the specific fluid and thermodynamic conditions, thus accounting for non-ideality effects. However, as noted in ISO 5167 itself, there are many gases and vapours for which no values for isentropic exponent have been published so far, particularly over a wide range of pressure and temperature. In such cases, the isentropic exponent is replaced by the ideal gas specific heats ratio, meaning that non-ideality effects are instead not taken into consideration. It is the Authors' opinion that the above practice, rooted in experimental results with three types of fluids only, could be very much improved by employing more modern computational tools like numerical simulations of the instrumentation which implement appropriate thermodynamic models, and verification in state-of-the-art dedicated wind tunnels operating with unconventional fluids, such as the TROVA. This would lead to an improvement of the instrumentation accuracy, enabling better plant regulation for power generation from ORCs and even in other key technologies for decarbonization involving unconventional fluids in non-ideal conditions, like heat pumps, CO_2 capture & storage and hydrogen applications.

Finally, supersonic testing was also carried out at total conditions with $Z_T \geq 0.66$ and Mach number $M \simeq 1.5$, typical of the flow downstream of ORC turbines cascades where Pitot tubes can be used for interstage losses measurement and blade cascade optimization. A simple Pitot tube (a total pressure probe) was employed to perform the first ever direct total pressure loss measurements across normal shock waves in non-ideal flows of siloxane MM vapors. Results were found to be in good agreement with theoretical shock losses predicted from the solution of conservation equations, setting the foundations for future directional pressure probe calibration and testing of blade cascades operating with such flows. The latter is routinely carried out for gas and steam turbines and, if applied to ORCs, would permit the experimental verification of numerical tools employed during the design process, for a deeper understanding of the fluid dynamics occurring within the turbomachinery. This would result in higher component and cycle efficiencies and, in turn, to a better usage of the available energy sources, with environmental and economic benefits.

For these reasons and as mentioned in the Introduction, an experimental campaign concerning supersonic blade cascade testing with MM vapor is undergoing on the TROVA [28], by employing the pressure probe methodologies here presented. The aim of the research is, precisely, the comparison between CFD simulations and measurements, with a focus on cascade total pressure losses experimentally measured by Pitot tubes and calculated numerically.

The present study is a first contribution to the field of experimental methodologies concerning pressure probes in non-ideal flows and, as such, it is limited to one type of probe, tested with one fluid in a specific range of thermodynamic conditions, and at a mild level of non-ideality in case of subsonic campaigns. For

this reason, future developments should involve testing in more non-ideal conditions, with other fluids of interest for ORCs and with directional pressure probes to study the influence on probe calibration coefficients for the determination of total and static pressures and flow angles. This would allow aerodynamic calibration of directional pressure probes in non-ideal conditions, unlocking reliable experimental characterization capabilities of the entire flow field downstream of blade cascades and in real ORC turbines, positively impacting on their optimal design and performance.

7. Acknowledgments

The authors wish to thank Ing. Gioele De Donati for his contribution to the experimental campaigns here reported. The present research was funded by ERC Proof of Concept Grant N. 875015, project *PROVA: Pitot PRobe for non-ideal compressible flows of organic VApors for renewable energy applications* under the Horizon 2020 Framework Programme, call: ERC-2019-PoC.

References

[1] P. Colonna, E. Casati, C. Trapp, T. Mathijssen, J. Larjola, T. Turunen-Saaresti, A. Uusitalo, Organic rankine cycle power systems: From the concept to current technology, applications, and an outlook to the future, Journal of Engineering for Gas Turbines and Power 137 (2015) 1–19. doi:10.1115/1.4029884.

[2] E. Macchi, M. Astolfi, Organic Rankine Cycle (ORC) Power Systems: Technologies and Applications, Woodhead Publishing, 2016.

[3] T. Tartière, M. Astolfi, A world overview of the organic rankine cycle market, Vol. 129, Elsevier Ltd, 2017, pp. 2–9. doi:10.1016/j.egypro.2017.09.159.

[4] C. Wieland, F. Dawo, C. Schifflechner, M. Astolfi, Market report on organic rankine cycle power systems: Recent developments and outlook. URL https://orc-world-map.org.

[5] A. Schuster, S. Karellas, E. Kakaras, H. Spliethoff, Energetic and economic investigation of organic rankine cycle applications, Applied Thermal Engineering 29 (8-9) (June 2009) 1809–1817.

[6] R. Bini, E. Manciana, Organic Rankine Cycle turbogenerators for combined heat and power production from biomass, in: Energy Conversion from Biomass Fuels, Current Trends and Future System, Munich, 1996.

[7] P. Bombarda, C. Invernizzi, C. Pietra, Heat recovery from diesel engines: a thermodynamic comparison between kalina and orc cycles, Applied Thermal Engineering 30 (1-2) (February 2010) 212–219.

[8] A. Duvia, S. Tavolo, Application of ORC units in the pellet production field: technical-economic considerations and overview of the operational results of an orc plant in the industry installed in madau (Germany), Tech. rep., Turboden s.r.l., Italy (2008).

[9] A. W. Adam, Organic Rankine Engines, in: Encyclopedia of Energy Technology and the Environment, Vol. 4, John Wiley & Sons, Inc., 1995.

[10] G. Angelino, M. Gaia, E. Macchi, A review of italian activity in the field of Organic Rankine Cycles, in: VDI Berichte - Proceedings of the International VDI Seminar, Zürich, Vol. 539, VDI Verlag, Düsseldorf, 1984.

[11] B. Saleh, G. Koglbauer, M. Wendland, J. Fischer, Working fluids for low-temperature organic rankine cycles, Energy 32 (7) (July 2007) 1210–1221.

[12] B. F. Tchanche, G. Papadakis, G. Lambrinos, A. Frangoudakis, Fluid selection for a low-temperature solar Organic Rankine Cycle, Applied Thermal Engineering 29 (11-12) (August 2009) 2468–2476.

[13] A. A. Lakew, O. Bolland, Working fluids for low-temperature heat source, Applied Thermal Engineering 30 (10) (July 2010) 1262–1268.

[14] C. Invernizzi, P. Bombarda, Thermodynamic performance of selected HCFS for geothermal application, Energy 22 (1997) 887–895.

[15] G. Angelino, C. Invernizzi, Cyclic methylsiloxanes as working fluids for space power cycles, ASME J. Sol. Energy Eng. 115 (1993) 130–137.

[16] U. Drescher, D. Brüggemann, Fluid selection for the organic rankine cycle (orc) in biomass power and heat plants, Applied Thermal Engineering 27 (1) (January 2007) 223–228.

[17] A. Romei, D. Vimercati, G. Persico, A. Guardone, Non-ideal compressible flows in supersonic turbine cascades, Journal of Fluid Mechanics 882 (2020) A121–A1226. doi:10.1017/jfm.2019.796.

[18] A. Spinelli, M. Pini, V. Dossena, P. Gaetani, F. Casella, Design, simulation, and construction of a test rig for organic vapors, Journal of Engineering for Gas Turbines and Power 135 (2013) 1–10. doi:10.1115/1.4023114.

[19] A. Head, C. D. Servi, E. Casati, M. Pini, P. Colonna, Preliminary design of the orchid: A facility for studying non-ideal compressible fluid dynamics and testing orc expanders, Vol. 3, 2016. doi:10.1115/GT2016-56103.

[20] F. Reinker, E. Y. Kenig, M. Passmann, S. A. D. Wiesche, Closed loop organic wind tunnel (clowt): Design, components and control system, Energy Procedia 129 (2017) 200–207. doi:10.1016/j.egypro.2017.09.158.
URL http://dx.doi.org/10.1016/j.egypro.2017.09.158

[21] M. C. Robertson, P. J. Newton, T. Chen, R. F. Martinez-Botas, Development and commissioning of a blowdown facility for dense gas vapours, American Society of Mechanical Engineers, 2019. doi:10.1115/GT2019-91609.

[22] T. Turunen-Saaresti, A. Uusitalo, J. Honkatukia, Design and testing of high temperature micro-orc test stand using siloxane as working fluid, Journal of Physics: Conference Series 755 (2016). doi:10.1088/1742-6596/755/1/011001.

[23] L. Zanellato, M. Astolfi, A. Serafino, D. Rizzi, E. Macchi, Field performance evaluation of orc geothermal power plants using radial outflow turbines, Energy Procedia 129 (2017) 607–614. doi:10.1016/j.egypro.2017.09.218.
URL http://dx.doi.org/10.1016/j.egypro.2017.09.218

[24] F. Reinker, R. Wagner, M. Passmann, L. Hake, S. A. D. Wiesche, Performance of a rotatable cylinder pitot probe in high subsonic non-ideal gas flows, 2020.

[25] D. Baumgärtner, J. J. Otter, A. P. Wheeler, The effect of isentropic exponent on supersonic turbine wakes, Proceedings of NICFD 2020 2C-2019 (2019) 1–6. doi:10.1115/GT2019-90251.

[26] D. Baumgärtner, J. J. Otter, A. P. S. Wheeler, The effect of isentropic exponent on transonic turbine performance, Journal of Turbomachinery 142 (2020) 1–10. doi:10.1115/1.4046528.

[27] Critical and Choking Mach Numbers for Organic Vapor Flows Through Turbine Cascades, Vol. Volume 4: Controls, Diagnostics, and Instrumentation; Cycle Innovations; Cycle Innovations: Energy Storage; Education; Electric Power of Turbo Expo: Power for Land, Sea, and Air, v004T06A003. arXiv:https://asmedigitalcollection.asme.org/GT/proceedings-pdf/GT2021/84966/V004T06A003/6757881/v004t06a003-gt2021-59013.pdf, doi:10.1115/GT2021-59013.
URL https://doi.org/10.1115/GT2021-59013

[28] M. Manfredi, G. Persico, A. Spinelli, P. Gaetani, V. Dossena, Design of experiments for supersonic orc nozzles in linear cascade configuration, in: Proceedings of the 6th International Seminar on ORC Power Systems, Technical University of Munich, 2021.

[29] ISO3966, Measurement of fluid flow in closed conduits: Velocity area method using pitot static tubes (2008).

[30] S. Gallarini, A. Spinelli, L. Lietti, A. Guardone, An improved method for the investigation of thermal stability of organic fluids, in: Proceedings of the 5th International Seminar on ORC Power Systems, Athens, 2019.

[31] L. Keulen, S. Gallarini, C. Landolina, A. Spinelli, P. Iora, C. Invernizzi, L. Lietti, A. Guardone, Thermal stability of hexamethyldisiloxane and octamethyltrisiloxane, Energy 165 (10 2018). doi:10.1016/j.energy.2018.08.057.

[32] A. Spinelli, G. Cammi, S. Gallarini, M. Zocca, F. Cozzi, P. Gaetani, V. Dossena, A. Guardone, Experimental evidence of non-ideal compressible effects in expanding flow of a high molecular complexity vapor, Experiments in Fluids 59 (2018) 1–16. doi:10.1007/s00348-018-2578-0.
URL http://dx.doi.org/10.1007/s00348-018-2578-0

[33] M. H. Zucrow, J. D. Hoffman, Gas dynamics: Multidimensional flow vol. 2 (1977).

[34] A. Guardone, A. Spinelli, V. Dossena, Influence of Molecular Complexity on Nozzle Design for an Organic Vapor Wind Tunnel, Journal of Engineering for Gas Turbines and Power 135 (Apr. 2013).

[35] M. Zocca, A. Guardone, G. Cammi, F. Cozzi, A. Spinelli, Experimental observation of oblique shock waves in steady non - ideal flows, Experiments in Fluids (2019) 1–12doi:10.1007/s00348-019-2746-x.
URL https://doi.org/10.1007/s00348-019-2746-x

[36] C. C. Conti, A. Fusetti, A. Spinelli, P. Gaetani, A. Guardone, Pneumatic system for pressure probe measurements in transient flows of non-ideal vapors subject to line condensation, Measurement 192 (2022) 110802. doi:10.1016/j.measurement.2022.110802.
URL https://linkinghub.elsevier.com/retrieve/pii/S0263224122001002

[37] R. Span, W. Wagner, Equations of state for technical applications. i. simultaneously optimized functional forms for nonpolar and polar fluids, International Journal of Thermophysics 24 (2003) 1–39. doi:10.1023/A:1022390430888.

[38] P. Colonna, T. P. van der Stelt, A. Guardone, Fluidprop: a program for the estimation of thermo physical properties of fluids (2004).

[39] P. Colonna, N. R. Nannan, A. Guardone, E. W. Lemmon, Multiparameter equations of state for selected siloxanes, Fluid Phase Equilibria 244 (2) (2006) 193–211. doi:10.1016/j.fluid.2006.04.015.

[40] P. Colonna, N. R. Nannan, A. Guardone, Multiparameter equations of state for siloxanes: [(CH3)3-Si-O1/2]2-[O-Si-(CH3)2]i=1,...,3, and [O-Si-(CH3)2]6, Fluid Phase Equilibria 263 (2) (2008) 115–130. doi:10.1016/j.fluid.2007.10.001.

[41] M. Thol, F. H. Dubberke, G. Rutkai, T. Windmann, A. Köster, R. Span, J. Vrabec, Fundamental equation of state correlation for hexamethyldisiloxane based on experimental and molecular simulation data, Fluid Phase Equilibria 418 (2016) 133–151. doi:10.1016/j.fluid.2015.09.047.

[42] M. Thol, F. H. Dubberke, E. Baumhögger, J. Vrabec, R. Span, Speed of Sound Measurements and Fundamental Equations of State for Octamethyltrisiloxane and Decamethyltetrasiloxane, Journal of Chemical & Engineering Data 62 (9) (2017) 2633–2648.

[43] ISO5167, Measurement of fluid flow by means of pressure differential devices inserted in circular cross-section conduits running full-part 1: General principles and requirements (2003).